

ATP-induced Pore Formation in the Plasma Membrane of Rat Peritoneal Mast Cells

PETER E. R. TATHAM and MANFRED LINDAU

From the Department of Physiology, University College London, University Street, London WC1E 6JJ, United Kingdom; and the Biophysics Group, Department of Physics, Freie Universität Berlin, Arnimallee 14, D-1000 Berlin, Federal Republic of Germany

ABSTRACT We have investigated the ATP-induced permeabilization of rat peritoneal mast cells using three different techniques: (a) by measuring uptake of fluorescent membrane and DNA marker dyes, (b) by voltage-clamp measurements using the patch-clamp technique, and (c) by measurements of exocytosis in response to entry of Ca^{2+} and $\text{GTP}\gamma\text{S}$ into permeabilized cells. In the absence of divalent cations cells become highly permeable at ATP concentrations as low as 3 μM . In normal saline containing 1 mM MgCl_2 and 2 mM CaCl_2 , dye uptake and electric conductance are detectable at 100 μM ATP corresponding to 4 μM ATP^{4-} . The permeabilization is half-maximal at an ATP^{4-} concentration of 5–20 μM with a Hill coefficient near 2. The ATP-induced whole-cell conductance at saturating ATP concentrations was 35–70 nS, exhibiting only weak cation selectivity. The activation is very fast with a time constant ≤ 65 ms. Pores which are large enough to allow for permeation of substances of 300–900 D are expected to have a unit conductance of ~ 200 –400 pS. However, in whole cells as well as outside-out patches, discrete openings and closings of channels could not be observed at a resolution of ~ 40 pS and the single-channel conductance obtained from noise analysis is ~ 2 –10 pS. Entry of Ca^{2+} into cells permeabilized with ATP stimulates exocytosis at low but not at high ATP concentrations indicating loss of an essential intracellular component or components at a high degree of permeabilization. This inactivation is removed when $\text{GTP}\gamma\text{S}$ is provided in the medium and this leads to enhanced exocytosis. The enhancement only occurs at high ATP concentrations. These results strongly suggest that the ATP-induced pores are of variable size and can increase or decrease by very small units.

INTRODUCTION

While the role of intracellular ATP is established, it also has a number of well recognized extracellular functions (see Gordon, 1986). Prominent among these are its actions as a modulator of smooth muscle contraction and relaxation (Burnstock, 1976) and as a neurotransmitter (Burnstock, 1972) or cotransmitter (Fedan et al.,

Address reprint requests to Dr. Manfred Lindau, Biophysics Group, Department of Biophysics, Freie Universität Berlin, Arnimallee 14, D-1000 Berlin, West Germany.

1981) at certain synapses. ATP exerts its excitatory and inhibitory effects on smooth muscle through membrane receptors termed P_2 purinoceptors (Burnstock, 1978) and these may also be involved in the activation of other cell types such as endothelial cells (Needham et al., 1987).

Another effect of extracellular ATP is its ability to create permeability lesions in the plasma membrane of a variety of cell types including mast cells (Cockcroft and Gomperts, 1979a; Bennett et al., 1981), macrophages (Steinberg et al., 1987), lymphocytes (Mustelin, 1987), hemopoietic stem cells (Whetton et al., 1988), and a variety of transformed epithelial cell lines (Heppel et al., 1985). Unlike the excitatory and inhibitory effects mentioned above which appear to be generated by MgATP, the agonist for permeabilization is free ATP (i.e., ATP^{4-}). This species interacts on mast cells with a receptor that exhibits a specificity that distinguishes it from P_2 purinoceptors (Tatham et al., 1988).

Very little is known about the physical and biochemical properties of these permeability lesions. They appear to be aqueous pathways and their formation is reversible. Removal of ATP^{4-} from solution by addition of excess Mg^{2+} causes the permeabilized cells to reseal (Gomperts, 1983), and this has provided a means of loading and trapping exogenous solutes within susceptible cells without loss of viability (Tatham and Gomperts, 1990).

An indication of the size of the holes generated in mast cells has been obtained from the molecular weights of solutes that can cross the plasma membrane. For instance, studies of the leakage of phosphate-containing cell metabolites (molecular weight in the range 80–300 D) suggest that pore size increases with ATP concentration, although lactate dehydrogenase (LDH) is retained (Cockcroft and Gomperts, 1979b). The largest molecules that have been loaded into mast cells using ATP have molecular weights in the range 600–1,000 D (Tatham, P. E. R., unpublished observations).

We have attempted to characterize the permeability lesions formed by ATP in the plasma membrane of single mast cells by observing their electrical properties using the patch-clamp technique and comparing the data with measurements of the uptake of fluorescent dyes that are normally impermeant. We have also tested the ability of the permeabilized cells to undergo exocytosis under similar ionic conditions. Our results show that ATP^{4-} generates high conductance pathways that exhibit only slight cation selectivity. Whole-cell conductance increases with the concentration of applied ATP and the pathways disappear rapidly on removal of the nucleotide. Our results suggest that the size of the aqueous pores formed by ATP increase continuously with $[ATP^{4-}]$.

MATERIALS AND METHODS

Cell Preparation

Rat mast cells were obtained by peritoneal lavage. For patch-clamp experiments 20–50 ml of saline were used, containing 143 mM NaCl, 5 mM KCl, 1 mM $MgCl_2$, 2 mM $CaCl_2$, 45 mM $NaHCO_3$, 0.4 mM Na_2HPO_4 , 8.3 mM glucose, and 10 mM HEPES-NaOH (pH 7.2–7.3). Aliquots of the aspirated cell suspension were layered onto glass coverslips set into the bottom of Petri dishes. These were kept at 37°C in a fully humidified atmosphere containing 8%

CO₂ for at least 30 min before use. Purified mast cells for secretion and dye uptake measurements were isolated from peritoneal washings by centrifugation through a density step of either bovine serum albumin (35% wt/wt, Path-O-Cyte 4; Miles Laboratories Ltd., Slough, UK), Ficoll (25% wt/vol) or Percoll (87.8% vol/vol; Pharmacia LKB, UK). The purified cells were then washed and resuspended in a buffered salt solution containing 140 mM NaCl, 5 mM KCl, 1 mM MgCl₂, 2 mM CaCl₂, 5.6 mM glucose, 1 mg/ml bovine serum albumin, and 20 mM HEPES (pH 7.2).

Patch Clamp

Standard patch-clamp techniques were used as described by Hamill et al. (1981). The command input of the patch-clamp amplifier (EPC-7; List Electronics, Darmstadt, FRG) operated in the voltage-clamp mode was controlled by a PDP11/73 computer with Cheshire Data Interface via the D/A converter. For continuous recording of the current the amplifier output was connected to a modified pulse code modulator (PCM 501 ES; Sony Corp.) with DC-coupled inputs and modified input and output filters. The modifications were based on a design that was generously provided by Dr. Fred Sigworth of Yale University. Data were stored on a conventional video recorder. For recording of the currents during voltage pulses the current output was directly sampled by the computer after filtering close to the nyquist frequency (LPF 902; Frequency Devices Inc., Haverhill, MA).

Conductance measurements were performed using the time domain technique described by Lindau and Neher (1988). In these experiments short pulses of -20 mV amplitude and 1.4–3 ms duration were given from a holding potential of 0 mV at time intervals between 20 ms and 1 s and the current responses without capacitance compensation were sampled by the computer. Provided the leakage conductance at the pipette-membrane seal is small compared with the access conductance (reciprocal of the resistance of the pipette-cell connection in the whole-cell configuration), analysis of the current responses yields accurate values of the true membrane conductance without using the series resistance compensation circuit of the amplifier. For this method it is only required that the conductance is approximately voltage independent within the 20-mV range of the pulse and that it does not change considerably during the 1.4–3-ms pulse duration. In some cases a variable seal conductance in parallel with the cell-access resistance combination was included in the equivalent circuit (see Lindau and Neher, 1988) and the capacitance was assumed to be constant. With this procedure changes of membrane conductance could be separated from changes of the leak conductance at the pipette-membrane seal.

Noise analysis of ATP-induced currents was performed using standard techniques (Anderson and Stevens, 1973). Segments of currents during voltage pulses to potentials of ± 30 –50 mV were sampled by the computer after low-pass filtering. Power spectra were calculated from typically 512 data points by an integer FFT (fast Fourier transform) routine. Typically 100 spectra obtained in the presence and absence of ATP were averaged and subtracted from each other. The mean of the ATP-induced current as well as its variance was also obtained as the difference of the values measured in the presence and absence of ATP.

The pipette solution contained 150 mM K-glutamate, 7 mM MgCl₂, 0.1 mM EGTA, 0.1 mM Na₂ATP, and 10 mM HEPES (pH 7.2). The external solution contained 140 mM NaCl, 5 mM KCl, 1 mM MgCl₂, 2 mM CaCl₂, and 10 mM HEPES (pH 7.2). Sufficient glucose was added (~ 25 mM) to bring the osmolality to 310 mosmol/liter.

ATP application during patch-clamp recordings presented major difficulties. When cells were monitored in the whole-cell configuration while the external medium was exchanged by bath perfusion the increase in membrane conductance was also frequently accompanied by severe deterioration of the pipette-membrane seal. Similarly, excised outside-out patches were usually destroyed with this method. In most cases we have thus used alternative methods

for adding ATP. In some experiments different volumes of a solution containing a high concentration of ATP in standard external saline were manually added to the periphery of the recording chamber with a pipette and the conductance was monitored until a new steady state was reached. The final concentration of ATP was then calculated from the estimated total volume of fluid in the recording chamber ($120 \pm 40 \mu\text{l}$). In other experiments the medium was changed by adding much larger quantities of ATP-containing saline (between 0.2 and 1 ml). The final concentration was again estimated using the initial volume given above. To measure the time course of the conductance increase and decrease upon addition and removal of ATP, 0.2 ml of a solution containing 3.16 mM ATP was added to the recording chamber as rapidly as possible. ATP was washed out by bath perfusion. The time required for the solution exchange was $\sim 1\text{--}3$ s as estimated from measurements of diffusion potential changes or dye washout from the recording chamber.

The liquid junction potential that develops at the pipette tip when it is immersed in the bath solution was determined to be 10–13 mV with our standard solutions. The potentials given here were not corrected for this junction potential, which reflects the different mobilities of the asymmetrically distributed ions. For large aqueous pores the relative mobilities are also expected to determine the relative pore permeabilities. For such a pore lacking any intrinsic selectivity filter, the correction for the liquid junction potential would thus lead to a reversal potential of ~ -10 mV, which simply reflects the different ion mobilities in water.

Dye Uptake and Fluorescence Measurements

Cell permeabilization was assessed by observing the uptake of either ethidium bromide, which binds to DNA, or 1-(4-trimethylammoniumphenyl)-6-phenyl-1,3,5-hexatriene (TMA-DPH), which binds to membrane surfaces. Both of these fluorescent dyes are cationic and cannot under normal conditions cross cell membranes. After permeabilization, dye is able to enter cells and bind to its respective target, giving rise to enhanced fluorescence emission. The method has been described previously (Tatham et al., 1988; Tatham and Gomperts, 1989). Briefly, equal volumes of cell suspension and dye solution were added to a continuously stirred cuvette in a Luminescence Spectrometer (LS5; Perkin-Elmer Corp., Norwalk, CT). The final cell concentration was $3 \times 10^5/\text{ml}$ and the dye concentrations were 25 μM (ethidium) and 200 nM (TMA-DPH). ATP was added 1 min later and the time course of the emission was recorded for 2–3 min using the following wavelengths: 310/580 nm (ethidium) and 340/475 nm (TMA-DPH). Increases in fluorescence after 100 and 60 s, respectively, were recorded and used as measures of the rate of dye uptake.

Secretion and LDH Assay

Histamine secretion was measured by adding typically 50 μl of cell suspension to a similar volume of medium containing ATP at an appropriate concentration. After incubation at room temperature for 20 min the reaction was quenched by adding ice-cold saline buffered with 10 mM K-phosphate (pH 7). The cells were then sedimented at 2,000 g at 4°C. Supernatants were assayed for histamine as described previously (Cockcroft and Gomperts, 1979a). LDH in the supernatants was determined spectrophotometrically by adding NADH (dihydropyridine adenine dinucleotide; 0.1 mM) and observing the decrease in absorbance (340 nm) after the addition of pyruvate (5 mM).

Estimation of the Concentrations of Ionic Species

The free concentrations of Ca^{2+} , Mg^{2+} , and ATP^{4-} were computed using a program based on the algorithm of Perrin and Sayce (1976). (This program is a modified version of CHELATE provided by Dr. Sherwin Lee of the University of Pennsylvania). The stability constants for ATP were obtained from Martell and Smith (1977) and Smith and Martell (1982).

Curve Fitting

The smooth curves in Figs. 1 *C* and 5 and the corresponding Hill equation parameters were obtained by a conventional nonlinear least-squares fit of Eq. 2 (see Results). Since in the patch-clamp experiments the local ATP concentration at the cell from which recordings were made had a much larger error than the measured conductance, the equation was inverted (ATP concentration as a function of conductance) and the parameters of this inverted equation were fit to the data. The results were only slightly different from those obtained by fitting the original equation.

Materials

TMA-DPH was purchased from Molecular Probes Inc. (Eugene, OR). Ethidium bromide and compound 48/80 were obtained from Sigma Chemical Co. (St. Louis, MO) and ATP was from Boehringer Mannheim Diagnostics, Inc. (Indianapolis, IN).

All patch-clamp, dye uptake, and secretion measurements were made at room temperature (18–24°C).

RESULTS

Measurements of Fluorescent Dye Uptake

Measurements of dye uptake into permeabilized cells were performed in the presence of Mg^{2+} and Ca^{2+} (plus bovine serum albumin to maintain viability, see Materials and Methods). Examples of the fluorescence traces obtained are shown in Fig. 1, *A* and *B* and these are similar to those observed previously in the absence of divalent ions (Tatham et al., 1988). Fig. 1 *C* shows the concentration dependence of the rate of the increase in fluorescence induced by ATP. Dye uptake is detectable at concentrations as low as 100 μM ATP corresponding to 4 μM ATP^{4-} , and the rate of increase in fluorescence reaches its maximum at between 300–600 μM ATP corresponding to 13–30 μM ATP^{4-} . (In the absence of divalents at pH 7.8 uptake is detectable at 1 μM ATP [$\sim 1 \mu M$ ATP^{4-}] and is maximal near 10 μM [Tatham et al., 1988]). Thus if we assume that membrane channels are opened by ATP^{4-} such that



where *C* and *O* correspond to the closed and open channel, respectively, then the degree of permeabilization *P* should follow the concentration dependence

$$P = P_{\max} \cdot [ATP^{4-}]^n / ([ATP^{4-}]^n + EC_{50}^n) \quad (2)$$

EC_{50} is the concentration at which the permeabilization is half-maximal. Since the maximum slope of the fluorescence increase should be directly proportional to *P*, this quantity can be used to determine EC_{50} as well as the Hill coefficient. The smooth lines in Fig. 1 *C* are least-squares fits to the data points according to Eq. 2. The corresponding parameters for ethidium bromide are $EC_{50} = 11 \pm 1 \mu M$ and $n = 1.6 \pm 0.2$. For TMA-DPH we obtain $EC_{50} = 6.2 \pm 0.5 \mu M$ and $n = 1.8 \pm 0.2$.

Patch-Clamp Experiments

When ATP was applied to mast cells voltage clamped in the whole-cell configuration, a very large increase of the membrane conductance was observed. Fig. 2 shows

the current recorded at a pipette potential of +30 mV. In the absence of ATP the recorded current is vanishingly small, which accords with the low incidence of ion channels in the plasma membrane of mast cells (Lindau and Fernandez, 1986). At the time indicated by the first arrow, 10 μ l of external saline containing 500 μ M ATP was added to the recording chamber as close as possible to the pipette tip. This induced a large outward current which in this particular experiment was nearly

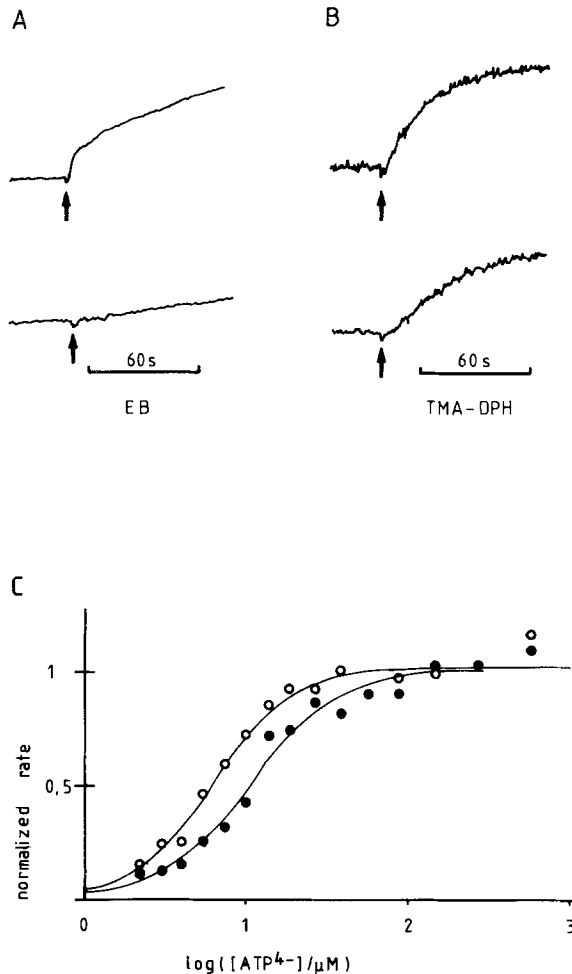


FIGURE 1. ATP-induced uptake of fluorescent dyes by mast cells in the presence of CaCl_2 (2 mM) and MgCl_2 (1 mM). *A* and *B* show time courses of the fluorescence emission from cells in the presence of ethidium bromide (25 μ M) and TMA-DPH (200 nM), respectively. ATP was added at the times indicated by the arrows to a final total concentration of 1 mM (*upper traces*) or 0.178 mM (*lower traces*). (Note that the abrupt increase in ethidium fluorescence that occurs after addition of 1 mM ATP (*A*) was also observed when no cells were present and is presumed to be due to an interaction between ATP and the dye. It was not observed at lower ATP concentrations (*B*) and where it was apparent it was subtracted from the signal before calculating the rate of dye uptake). *C* shows the dependence of the rate of dye uptake (in arbitrary units) on $[\text{ATP}^{4-}]$ (*filled circles*, ethidium bromide; *open circles*, TMA-DPH). For further details see Materials and Methods.

2 nA. During the next 60 s the current declined to a value of \sim 40 pA. A second addition of ATP elicited a similar response. Since in this experiment the contents of the chamber were not stirred, the time taken for the current to reach its maximum value probably reflects the time required for ATP to diffuse to the membrane of the cell being recorded from. Similarly, the subsequent decline in current is likely to be an effect of the dilution of ATP near the cell as diffusional equilibrium is achieved throughout the whole chamber.

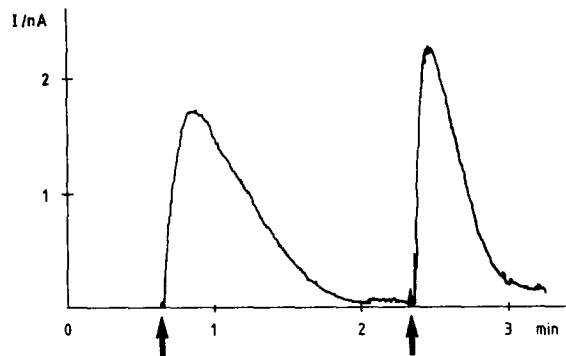


FIGURE 2. Whole-cell current measured in a mast cell at a holding potential of +30 mV. At the times indicated by the arrows 10 μ l of saline containing 500 μ M ATP were added as close as possible to the pipette tip.

Since the currents measured in the presence of ATP are very large, the considerable voltage drop across the finite access resistance of the pipette-cell connection has to be accounted for. The series resistance compensation assumes a constant pipette-cell resistance. In the experiments shown here large variations of the series resistance occurred in many cases making it important to distinguish clearly between changes in membrane conductance and changes in series resistance. We have therefore measured the current responses to short (1.4–3 ms) voltage pulses without capacitance compensation. Analysis of these current signals generates exact values of the membrane conductance and access resistance without using the series resistance compensation circuit (Lindau and Neher, 1988).

To investigate the concentration dependence of the effect of ATP, cells were monitored in the whole-cell configuration while the external ATP concentration was changed. Since the quality of the pipette-membrane seal always decreased markedly when ATP was present and was completely lost in most experiments the concentration dependence could only be measured in three cells. Fig. 3 shows the conductance observed in the presence of ATP at concentrations between 0.1 and 2 mM. Between the applications of the different concentrations of ATP, the chamber was washed with external saline (by bath perfusion) and this reduced the conductance almost to the initial level. (Note that after the wash-out following the second addition of ATP a significant leakage current remained, indicating decreased seal resis-

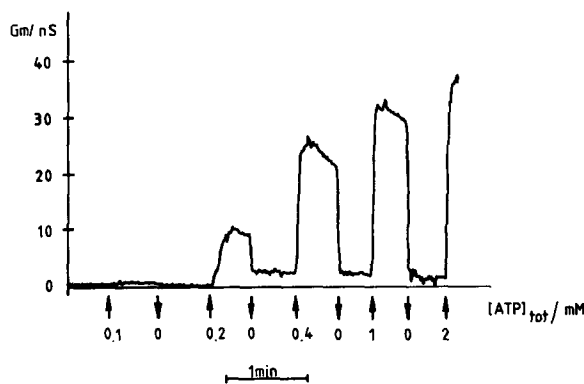


FIGURE 3. Whole-cell membrane conductance reconstructed from current signals evoked by 2-ms voltage pulses from 0 to -20 mV. At the times indicated by upward arrows the chamber was perfused with 1 ml of ATP containing saline at the indicated concentrations. At the downward arrows the chamber was washed with ATP-free saline using the bath perfusion system.

tance. The seal was lost at the end of the recording shown in this figure). On several occasions outside-out patches were pulled from the attached cell after ATP was washed off. In all cases the apparent conductance remained unchanged even though the area of such a patch is only a few percent of that of the whole plasma membrane, which indicates that the irreversible conductance change was due to decreased seal resistance. These results clearly demonstrate that the ATP-induced pores close completely when ATP is removed and any irreversible conductance is merely due to damage to the seal. Even when only a small drop of ATP-containing saline was added to minimize any possible mechanical forces on the seal, the seal resistance decreased to a few $M\Omega$ in $> 90\%$ of the experiments.

To demonstrate that the observed conductance changes are induced by ATP^{4-} rather than $MgATP^{2-}$ or $CaATP^{2-}$ we also performed patch-clamp experiments in the absence of divalent cations. Fig. 4 illustrates such an experiment. After the whole-cell configuration was established, the cell was washed with divalent free saline containing 150 mM NaCl, 5 mM KCl, 10 mM HEPES/NaOH pH 7.2, 100 μM

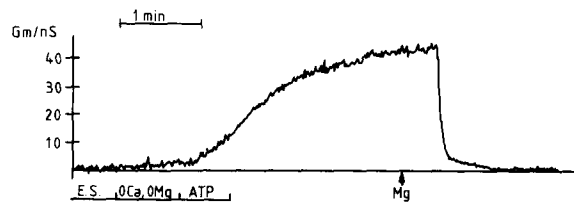


FIGURE 4. ATP-induced conductance changes in the absence of divalent cations. The recording chamber was perfused as indicated by the bars with (a) normal external saline (E.S.), (b) saline containing neither Mg^{2+} nor Ca^{2+} and (c) divalent-free saline containing 3 μM ATP, after which the perfusion was halted. At the time of the arrow 2 μl 1 M $MgCl_2$ solution were added to the recording chamber at some distance of the cell.

EGTA, 100 μM EDTA. The solution was subsequently exchanged for a solution containing 3 μM ATP which induced a large increase of membrane conductance. At the time of the arrow $MgCl_2$ was added at some distance from the cell to a final concentration of ~ 15 mM. After a delay due to the diffusion time required for the Mg^{2+} to reach the cell membrane, the conductance decreased rapidly suggesting that the observed conductance changes are induced by the tetrabasic form ATP^{4-} .

To increase the concentration of ATP^{4-} in the cell interior to 100 μM (i.e., ~ 80 -fold) we increased ATP in the pipette solution to 1.8 mM and reduced $MgCl_2$ to 3 mM. Under these conditions the membrane conductance remained below 300 pS for more than 10 min. We thus conclude that intracellular ATP^{4-} does not create pores in the plasma membrane of mast cells.

The normalized reversible ATP-induced conductance changes measured in two different cells are plotted as a function of $[ATP^{4-}]$ in Fig. 5. A least-squares fit of Eq. 2 (smooth line) yields $EC_{50} = 19 \pm 2 \mu M$ and $n = 2.1 \pm 0.3$. In another cell, which had degranulated during an ATP application before the concentration dependence

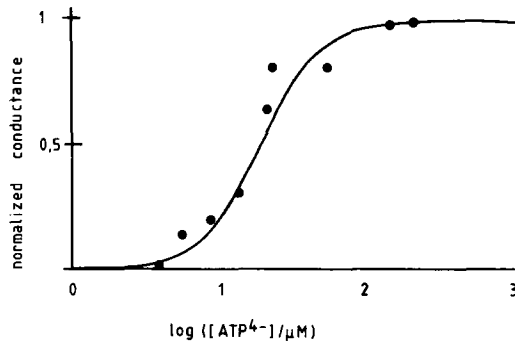


FIGURE 5. Concentration dependence of the ATP-induced conductance. Data from two cells were normalized with respect to the maximal conductance. The solid line is a least-squares fit of Eq. 2 yielding $EC_{50} = 19 \pm 2 \mu\text{M}$ and $n = 2.1 \pm 0.3$.

was measured, we obtained $EC_{50} = 43 \pm 8 \mu\text{M}$ and $n = 1.3 \pm 0.3$ (graph not shown). The concentration shift here could be caused by granule matrices which cover the membrane surface after degranulation. Although this is unlikely to materially affect the surface potential the very substantial negative charge which they carry will act to reduce the local concentration of ATP in the vicinity of the cell surface.

Fig. 6 shows the time course of the conductance change obtained upon adding 0.2 ml of a solution containing 3.16 mM ATP to the recording chamber. The final concentration was estimated to be ~ 2 mM corresponding to $190 \mu\text{M ATP}^{4-}$. The conductance increased with a rise time ($t_{10/90}$) of 140 ms, a value reflecting the time required for the concentration change in the recording chamber. Assuming an exponential time course for the opening of the channels yields a time constant of < 65 ms, which thus is an upper limit for the ON time of channel opening. After 10 s the ATP was washed out by bath perfusion, which requires 1–3 s. Again the conductance decrease was found to follow approximately the time course of the expected concentration change.

The current-voltage relationship of the ATP-induced conductance was measured by giving 100 ms pulses from a holding potential of 0 mV in the presence of ~ 2 mM ATP (total). The currents measured during pulses to potentials between -100 and $+60$ mV are shown in Fig. 7 A. They exhibit no pronounced time dependence. To construct the current-voltage relationship shown in Fig. 7 B we have thus averaged the current during each individual pulse. The current-voltage dependence is nearly ohmic with only weak inward rectification. This phenomenon is not unexpected. Since the pipette solution contained 7 mM MgCl_2 and Mg^{2+} may also permeate

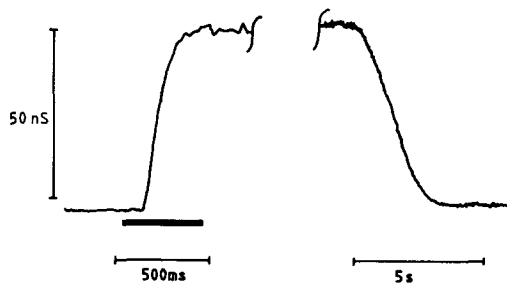


FIGURE 6. Time course of the ATP-induced whole-cell conductance change. A -20 mV pulse was given every 20 ms. During the time indicated by the horizontal bar (left) $200 \mu\text{l}$ of saline containing 3.16 mM ATP were added to the recording chamber. The washout of ATP (right bar) was performed by the perfusion system.

through the ATP-induced pores (see below for pore selectivity), the concentration of Mg^{2+} at the extracellular membrane surface will be higher at more positive potentials. The elevated Mg^{2+} concentration will accordingly reduce the concentration of ATP^{4-} .

With our standard solutions the reversal potential was always between 0 and -5 mV. To investigate if the ATP-induced pores exhibit any selectivity for cations or anions we used a modified external saline where NaCl and KCl were reduced by a factor of five. (The osmolarity was adjusted to 310 mosmol/liter by including ~ 250 mM glucose.) For a channel selectively permeable to monovalent cations this should

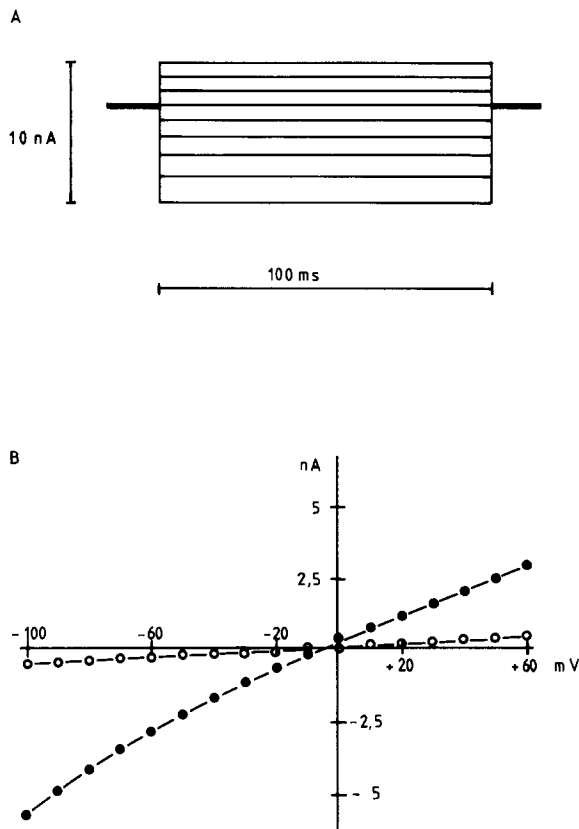


FIGURE 7. (A) Whole-cell currents measured during 100-ms voltage pulses given from 0 mV to potentials between -100 and $+60$ mV. (B) Current-voltage relationship constructed by averaging the current during the 100-ms pulse period. *Filled symbols*: in the presence of ~ 2 mM ATP total. *Open symbols*: after washing the chamber with ATP-free saline.

result in a shift of the reversal potential by 41 mV in the negative direction. With this solution we observed a reversal between -15 and -9 mV, which indicates slight cation selectivity. During these experiments we observed that the reversal was already shifted to -5 to -8 mV when the pipette was pressed against the cell membrane before the seal was established. Such a pronounced shift was not observed with our standard saline. This phenomenon can be attributed to the negative surface charge of the membrane which necessarily leads to an increased concentration of cations and to a decreased concentration of anions at the membrane surface at low ionic strength (Chandler et al., 1965). The shift of the reversal potential

by ~ -10 mV which we observed in the dilution experiment is very close to that estimated for the effect of the surface potential on the relative permeabilities following the treatment of Chandler et al. (1965).

To determine the conductance of individual pores we have attempted to resolve unitary events of channel opening or closing in excised outside-out patches. Such an experiment is illustrated in Fig. 8 A. An outside-out patch was formed and the current was measured at a pipette potential of +50 mV. Before ATP application the

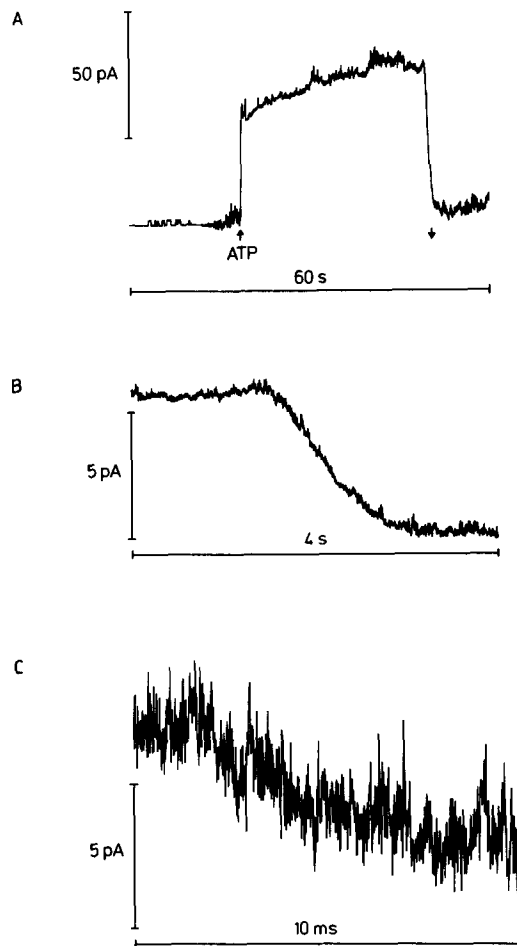


FIGURE 8. Current recorded from an outside-out patch at a holding potential of +50 mV. At the first arrow (upward) $10 \mu\text{l}$ of a solution containing 4 mM ATP were added close to the pipette tip. At the second arrow (downward) the chamber was washed with ATP-free saline. In *B* and *C* the current during washout is displayed at higher time resolution. The current was recorded on tape after filtering at 10 kHz. The traces shown here were filtered during replay at 20 Hz (*A*), 500 Hz (*B*), and 5 kHz (*C*).

trace shows only a few single-channel openings with a unitary current of ~ 2 pA which may represent the calcium-dependent cation channel of the mast cell membrane (Lindau and Fernandez, 1986). At the first arrow (upward) $10 \mu\text{l}$ of normal saline containing 4 mM ATP were added to the bath close to the pipette tip. The small noise preceding the addition of ATP is due to an electrical artifact that occurred when the pipette tip was held close to the recording electrode. The addition of ATP generated an outward current of ~ 50 pA. For a reversal between 0 and

–5 mV this corresponds to a conductance of ~1 nS. To determine the number of channels contributing to this conductance we examined the current decrease during the wash-out of ATP (second arrow, downward). This part of the trace is shown at increasing time resolution in Fig. 8, *B* and *C*. The decrease is apparently continuous. If discrete open-to-closed transitions are hidden in these traces, then the amplitude resolvable at 5 kHz bandwidth is < 2 pA, which corresponds to a unit conductance below 40 pS.

To examine the unit conductance further we have applied the methods of noise analysis to currents measured in whole cells and outside-out patches in the presence of ATP at different concentrations. At low ATP the unit conductance calculated from the variance/mean ratio was 2–10 pS. As expected for a channel mechanism, the variance/mean ratio decreased to ~0.2 pS at high ATP concentrations. However, the frequency spectra were dominated by $1/f$ noise and did not exhibit a clear cut-off frequency up to our measuring bandwidth of 10 kHz.

These results suggest that either the unit conductance is smaller than ~10 pS or that the pores exhibit very fast flickering beyond 10 kHz.

Stimulation of Exocytosis

ATP can indirectly stimulate mast cells to undergo exocytosis in the presence of physiological concentrations of Ca^{2+} and Mg^{2+} (Sugiyama, 1971; Dahlquist and Diamant, 1974) by allowing entry of Ca^{2+} ions through permeability lesions (Cockcroft and Gomperts, 1980). However, cells treated in this way lose their ability to secrete histamine at high levels of ATP (Cockcroft and Gomperts, 1980). It was originally thought that this inhibition was due to excessive Ca^{2+} within the cytosol of permeabilized cells. However, it is also possible that the lesions formed at higher concentrations of ATP are larger, causing the loss of essential solutes that are retained at lower concentrations of the nucleotide. Fig. 9 *A* shows the secretory response of mast cells treated with ATP in the presence of Ca^{2+} and Mg^{2+} for 20 min. Histamine secretion is detectable at 60 μM ATP (2.4 μM ATP^{4-}) and increases to a maximum at 130 μM (5.3 μM ATP^{4-}). Thereafter the response decreases to background levels before increasing again at 3 mM ATP (0.5 mM ATP^{4-}). Note that although $[\text{Ca}^{2+}]$ and $[\text{Mg}^{2+}]$ begin to fall at $[\text{ATP}] > 0.5$ mM, free $[\text{Ca}^{2+}]$ is always > 0.4 mM as illustrated in Fig. 9 *B*.

To investigate the possibility that leakage of essential metabolites is responsible for the inhibition, the nonhydrolyzable GTP analogue, $\text{GTP}\gamma\text{S}$ (10 μM), was provided in the medium during permeabilization. A typical experiment is illustrated in Fig. 9 *C*. The effect of $\text{GTP}\gamma\text{S}$ is to remove the inhibitory phase of the response curve almost completely, demonstrating that the cells at the higher ATP levels used in this study are still capable of undergoing exocytotic secretion. Since extracellular GTP does not permeabilize or activate mast cells (Cockcroft and Gomperts, 1980) it also indicates that loss of GTP is the likely cause of the inhibition of secretion at higher ATP levels.

In the absence of $\text{GTP}\gamma\text{S}$ and at the highest concentrations of ATP there is also evidence of recovery from the inhibition (Fig. 9 *A*). This result agrees well with the observation that MgATP at concentrations above 0.5 mM supports secretion due to 10 μM Ca^{2+} in mast cells permeabilized with streptolysin O (Howell and Gomperts,

1987). LDH release from ATP-treated cells was not significantly different from that measured in the absence of ATP (< 8%).

DISCUSSION

We have investigated the permeabilization of rat peritoneal mast cells by ATP using three different techniques that provide complementary information: (a) detection

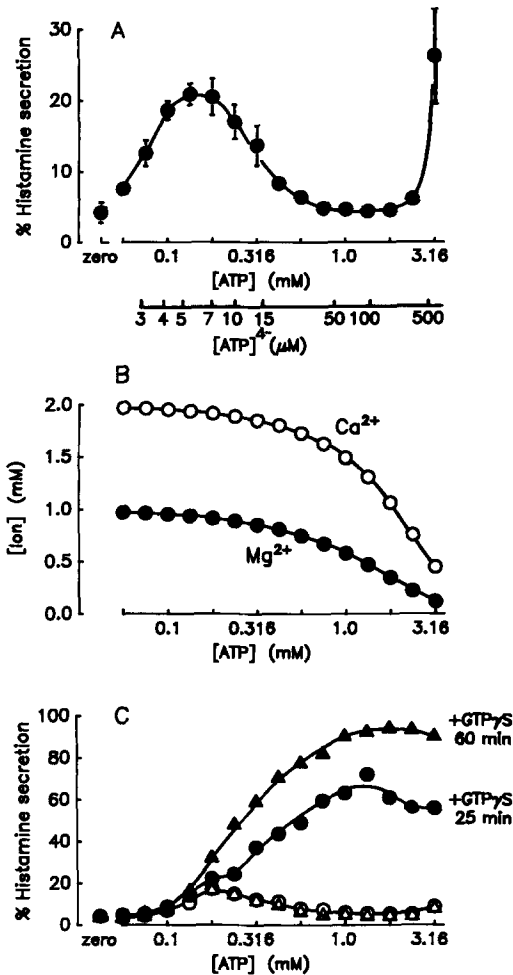


FIGURE 9. ATP-induced secretion and the effect of GTP γ S. A shows the concentration dependence of histamine secretion (at 20 min) from mast cells exposed to ATP in medium containing 2 mM CaCl₂ and 1 mM MgCl₂ at room temperature (bars indicate SEM, $n = 4$ experiments). Calculated concentrations of ATP⁴⁻ are indicated on the abscissa and the free concentrations of Ca²⁺ (open circles) and Mg²⁺ (filled circles) are shown in B. C shows the effect of the presence of GTP γ S (10 μ M) on ATP-induced secretion measured after 25 min (filled circles) and 60 min (filled triangles). The open symbols indicate the corresponding control experiments in which GTP γ S was omitted.

of the uptake of membrane- or DNA-staining fluorescent dyes, (b) patch-clamp conductance measurements, and (c) measurement of secretion after stimulation by the introduction of Ca²⁺ and GTP γ S into permeabilized cells. The patch-pipette experiments described here show that ATP permeabilization can be directly observed by voltage-clamp measurements. In the absence of divalent cations a large increase of membrane conductance to ~40 nS was observed at an ATP concentration of 3 μ M, which is reversed upon addition of excess Mg²⁺, indicating that ATP⁴⁻ is the active

species. In the presence of millimolar concentrations of Ca^{2+} and Mg^{2+} , the active species ATP^{4-} is present in solution only as a minor equilibrium component. Consequently, in order to study its effects, it has been convenient in the past to use media lacking divalent cations. However, it is not necessary to adopt these conditions for effective permeabilization. In order to make useful comparisons between the data from each experimental approach, we have used similar media containing Ca^{2+} and Mg^{2+} in most experiments (see Materials and Methods). The maximum membrane conductance that can be induced in a single mast cell under these conditions is 35–70 nS and is fully reversible. The saturating conductance in degranulated cells was not significantly higher suggesting that such ATP receptors are not present on the inner side of the granular membranes. The rate at which pores are opened in the mast cell membrane is so rapid that it is beyond the time resolution of any of the techniques that we have applied. Patch-clamp measurements reveal an increase in conductance that occurs with a time constant of < 65 ms. Similarly the closing time (which could not be determined with the same resolution) was also found to be rapid (< 1 s). The permeabilizing and resealing events are therefore very fast.

For a given molecular weight the maximal rate of dye uptake should be proportional to the degree of permeabilization. However, the compounds that we have used possess similar molecular weights but give rise to quite different rates of increase of fluorescence (Fig. 1, *A* and *B*), ethidium taking approximately ten times longer than TMA-DPH to reach a steady-state value. The dyes themselves are unlikely to interfere with the permeabilization process, therefore other factors intrinsic to them must be responsible for this difference. At a certain degree of permeabilization the rate of increase in emission will be limited by the rate of diffusion of the dye through the cell interior, and in the case of ethidium on its rate of incorporation into the nucleus. Eq. 2 implies that the rate of uptake should become very high as the degree of permeabilization becomes large. It is clear from the data in Fig. 1 that at a high degree of permeabilization (higher [ATP]), the development of the fluorescence signal from ethidium is slower than that of TMA-DPH, which indicates that other factors limit the rate of fluorescence increase.

In the case of TMA-DPH, the high affinity for membrane surfaces (Prendergast et al., 1981) may lead to an effective intracellular diffusion coefficient that is considerably lower than that expected for a molecule of 300 D. A similar effect has been observed in a study of the intracellular diffusion of didansylcystine (a similar dye) in retinal rod outer segments (Hochstrate and Rüppel, 1980). The strong binding of this substance to membranes and the abundance of intracellular membrane within the preparation led to an observed diffusion velocity that was 1/1,000 of that in solution. The mast cell is densely packed with secretory granules, providing membranes that could act in a similar way to slow the movement of TMA-DPH within the cell and consequently to limit its rate of entry. Ethidium, on the other hand, does not have a strong affinity for membranes, but nevertheless has to diffuse through the restricted cytoplasm to its target in the nucleus. Thus for both dyes the rate of fluorescence increase at high degrees of permeabilization would not be limited simply by pore size or number, but would also be affected by rather slow diffusion rates within the cell. This view is supported by the finding that the leakage rate of 3-phosphoglyceratekinase and even LDH from mast cells permeabilized with strep-

tolysin O is comparable to the rate of fluorescence increase obtained from TMA-DPH uptake (Gomperts et al., 1987). By comparing diffusion coefficients (based on protein molecular weights of ~40 and ~150 kD, respectively, the dyes would be expected to enter the cells at about six times the rate of protein leakage. In spite of these complications, the curves relating the rate of uptake of ethidium and TMA-DPH to the concentration of ATP^{4-} are quite similar, the calculated EC_{50} values differing by a factor of 1.8, a difference that we do not consider significant. The concentration dependence of the conductance changes, which directly reflect membrane permeability, yields an EC_{50} value that is about twofold higher than those obtained using the fluorescent dyes. However, rats from a different source were used for these experiments and the external saline lacked bovine serum albumin, so that although this disparity may reflect the above differences in the mechanism by which the methods probe permeability, it is equally likely to be caused by experimental variations. The Hill coefficients for permeabilization obtained from dye uptake and patch-clamp conductance measurements are ~2 and this could be taken as evidence that binding of two ATP^{4-} molecules is required to open a channel.

The ATP-induced opening of pores in the membrane can be observed using a patch pipette in fully dialyzed cells as well as in excised outside-out patches. The initiation of permeabilization thus requires only components present in the plasma membrane and does not involve any cytosolic substances. The membrane conductance is not affected by elevating the intracellular ATP^{4-} concentration to ~100 μM . This strongly suggests that the permeabilizing activity of ATP is exerted exclusively by binding to receptors on the extracellular side of the plasma membrane.

From experiments with outside-out patches and by noise analysis we found that the unit conductance is certainly < 40 pS and may even be below 10 pS, if the recording bandwidth of 5–10 kHz was sufficient. From the relations between diffusion coefficient, hydrated molecular radius, molecular weight and partial molar volume the size of organic molecules with low molecular weight can be estimated (Longworth, 1952, 1953). For substances with molecular weights of ~300 D (such as ethidium or TMA-DPH) a diameter of ~1.0 nm is obtained and for compounds with molecular weights up to 900 D the size should be ~1.4 nm. For a membrane 7 nm thick an aqueous pore of this size would have an electrical conductance of ~200 or ~400 pS, respectively, with our standard solutions. Transitions of this size would be clearly evident in current records from outside-out patches such as that of Fig. 8. How can this discrepancy be explained? We consider it most likely that the pores are of variable size. Such a heterogeneous distribution of channels could either be static or dynamic. For a static distribution the data presented here suggests that a population exists having unit conductances up to ~300 pS but with a mean conductance as low as 10 pS. For channels with well-defined agonist specificity (Tatham et al., 1988) it is difficult to imagine fixed structures that could have unit conductances varying by a factor of 30 or more. Such variability arises more likely from dynamic fluctuations. If we assume that individual channels, activated by two ATP molecules, exhibit such fluctuations independent of agonist concentration, these fluctuations should increase in proportion to the number of activated channels. The fluctuations should thus increase in proportion to the mean current with increasing ATP concentration. However, the variance/mean ratio appears to decrease at increasing ATP concen-

tration suggesting that the channel fluctuations decrease. This finding supports the idea that the size of an individual pore varies with the ATP concentration. The size of the pores may change in very small steps, as they expand or contract, involving conductance changes of < 10–40 pS. The Hill coefficient of 2 would then suggest that two ATP⁴⁻ molecules are required to cross-link an additional element into an existing pore. We thus consider the individual pore as a macroscopic system vibrating among many states which could generate the observed 1/*f* noise. Alternatively, discrete openings may not be detectable as a consequence of very fast flickering of the ATP-induced pores with open times shorter than ~50 μs, which is the limit of resolution in the present experiments. This cannot be excluded since the kinetics of the response to the addition and removal of ATP could not be resolved and a clear cut-off frequency was not observed in the noise spectra.

Measurements of exocytotic secretion induced by ATP support a mechanism based on a variable pore size. Mast cells permeabilized with streptolysin-O will undergo exocytosis when provided with the two intracellular effectors, Ca²⁺ and GTP (or GTP analogue). The combination of these two agents is both necessary and sufficient for secretion (Gomperts et al., 1987; Gomperts and Tatham, 1988). ATP activates mast cells by permitting the entry, through pores, of Ca²⁺ ions, but it is clear from Fig. 9 that the inactivation that occurs at the higher concentrations of ATP is removed when the nonhydrolyzable GTP analogue GTPγS is provided. The effect of this nucleotide increases with increasing ATP concentration, but it has little effect at concentrations of ATP⁴⁻ below ~5 μM. We conclude that between 2.5 and 5 μM ATP⁴⁻, the pores are large enough to permit the entry of Ca²⁺ but too small to allow significant loss of nucleotides such as GTP, enabling exocytosis to occur. At higher ATP concentrations the leakage of larger molecules from the cells becomes possible, allowing nucleotides to escape, with the consequence that exocytosis is no longer supported. When GTPγS is provided, secretion is enhanced only when the cells are sufficiently permeabilized to allow its entry. Below ~5 μM ATP⁴⁻, GTPγS cannot enter the cells and consequently cannot affect secretion.

Further evidence for an increase in pore size with increasing ATP concentration was obtained from observations of the leakage of phosphorylated metabolites from ATP-treated mast cells (Cockcroft and Gomperts, 1979*b*). In the presence of divalent cations 1.4 μM ATP⁴⁻ permitted the efflux of inorganic phosphate. Above 2.9 μM, sugar phosphates also leaked from the cells and at 8.6 μM ATP⁴⁻ nucleotide loss was observed. These values (obtained at 37°C) are in agreement with the data of Fig. 9. Note that when divalent cations are omitted from the medium, ATP was effective at lower concentrations (Cockcroft and Gomperts, 1980), nucleotide leakage commencing at 1 μM ATP⁴⁻ and becoming maximal at 3 μM, which implies that the divalent cations may have a protective effect upon the cells. This is supported by our observation that 3 μM ATP induces a large increase in the membrane conductance in the absence of divalent cations.

Note added in proof: High conductance pathways induced by extracellular ATP with at least partially similar properties were recently also observed in patch-clamp experiments on macrophages (Buisman, H. P., T. H. Steinberg, J. Fischberg, S. C. Silverstein, S. A. Vogelzang, C. Ince, D. L. Ypey, and P. C. J. Leigh. 1988. *Proceedings of the National Academy of Sciences*. 85:7988–7992).

We wish to thank Dr. Fred Sigworth who generously provided the basic design of the PCM modifications and J. Kleindienst who installed the modifications. We thank Stefanie Wolgast for preparing most of the figures. We also thank Oliver Nüße for his help with some of the experiments and comments on the manuscript, and also Bastien Gomperts and Shamshad Cockcroft for their helpful advice.

This work was supported by the Deutsche Forschungsgemeinschaft within the Sonderforschungsbereich "Gerichtete Membranprozesse" Teilprojekt B6 (to M. Lindau) and by a grant from the Wellcome Trust to B. D. Gomperts.

Original version received 13 January 1989 and accepted version received 25 May 1989.

REFERENCES

- Anderson, C. R., and C. F. Stevens. 1973. Voltage clamp analysis of acetylcholine-produced end-plate current fluctuations at frog neuromuscular junction. *Journal of Physiology*. 235:655–691.
- Bennett, J. P., S. Cockcroft, and B. D. Gomperts. 1981. Rat mast cells permeabilised with ATP secrete histamine in response to calcium ions buffered in the micromolar range. *Journal of Physiology*. 317:335–345.
- Burnstock, G. 1972. Purinergic nerves. *Pharmacological Reviews*. 42:500–581.
- Burnstock, G. 1976. Purinergic receptors. *Journal of Theoretical Biology*. 62:491–503.
- Burnstock, G. 1978. A basis for distinguishing two types of purinergic receptor. In *Cell Membrane Receptors for Drugs and Hormones: A Multidisciplinary Approach*. R. W. Straub and L. Bolis, editors. Raven Press, NY. 107–118.
- Chandler, W. K., A. L. Hodgkin, and H. Meves. 1965. The effect of changing the internal solution on sodium inactivation and related phenomena in giant axons. *Journal of Physiology*. 180:821–836.
- Cockcroft, S., and B. D. Gomperts. 1979a. Activation and inhibition of calcium dependent histamine secretion by ATP ions applied to rat mast cells. *Journal of Physiology*. 296:229–243.
- Cockcroft, S., and B. D. Gomperts. 1979b. ATP induces nucleotide permeability in rat mast cells. *Nature*. 279:541–542.
- Cockcroft, S., and B. D. Gomperts. 1980. The ATP⁴⁻ receptor of rat mast cells. *Biochemical Journal*. 188:789–798.
- Dahlquist, R., and B. Diamant. 1974. Interaction of ATP and calcium on the rat mast cell: effect on histamine release. *Acta Pharmacologica et Toxicologica*. 34:368–384.
- Fedan, J. S., G. K. Hogaboom, J. P. O'Donnell, J. Colby, and D. P. Westfall. 1981. Contribution by purines to the neurogenic response of the vas deferens of the guinea pig. *European Journal of Pharmacology*. 9:41–53.
- Gomperts, B. D. 1983. Involvement of guanine nucleotide-binding protein in the gating of Ca²⁺ by receptors. *Nature*. 306:64–66.
- Gomperts, B. D., S. Cockcroft, T. W. Howell, O. Nüße and P. E. R. Tatham. 1987. The dual effector system for exocytosis in mast cells: obligatory requirement for both Ca²⁺ and GTP. *Bio-science Reports*. 7:369–381.
- Gomperts, B. D., and P. E. R. Tatham. 1988. GTP-binding proteins in the control of exocytosis. In *Molecular Biology of Signal Transduction*. Cold Spring Harbor Symposium on Quantitative Biology 53. M. Wigler, J. R. Feramisco, and J. D. Watson, editors. 983–992.
- Gordon, J. L. 1986. Extracellular ATP: effects, sources and fate. *Biochemical Journal*. 233:309–319.
- Hamill, O. P., A. Marty, E. Neher, B. Sakmann, and F. J. Sigworth. 1981. Improved patch-clamp techniques for high-resolution current recording from cells and cell-free membrane patches. *Pflügers Archiv*. 391:85–100.

- Heppel, L. A., G. A. Weisman, and I. Friedberg. 1985. Permeabilization of transformed cells in culture by external ATP. *Journal of Membrane Biology*. 86:189–196.
- Hochstrate, P., and H. Rüppel. 1980. On the evaluation of photoreceptor properties by micro-fluorimetric measurements of fluorochrome diffusion. *Biophysics of Structure and Mechanism*. 6:125–138.
- Howell, T. W., and B. D. Gomperts. 1987. Rat mast cells permeabilized with streptolysin O secrete histamine in response to Ca^{2+} at concentrations buffered in the micromolar range. *Biochimica et Biophysica Acta*. 927:177–183.
- Lindau, M., and J. M. Fernandez. 1986. A patch-clamp study of histamine-secreting cells. *Journal of General Physiology*. 88:349–368.
- Lindau, M., and E. Neher. 1988. Patch-clamp techniques for time-resolved capacitance measurements in single cells. *Pflügers Archiv*. 411:137–146.
- Longworth, L. G. 1952. Diffusion measurements, at 1°, of aqueous solutions of amino acids, peptides and sugars. *Journal of the American Chemical Society*. 74:4155–4159.
- Longworth, L. G. 1953. Diffusion measurements, at 25°, of aqueous solutions of amino acids, peptides and sugars. *Journal of the American Chemical Society*. 75:5705–5709.
- Martell, A. E., and R. M. Smith. 1977. Critical Stability Constants. Vol 3. Plenum Publishing Co., New York. 435 pp.
- Mustelin, T. 1987. GTP dependence of the transduction of mitogenic signals through the T3 complex in T lymphocytes indicates the involvement of a G-protein. *FEBS Letters*. 213:199–203.
- Needham, L., N. J. Cusack, J. D. Pearson, and J. L. Gordon. 1987. Characteristics of the P_2 purinoreceptor that mediates prostacyclin production by pig aortic endothelial cells. *European Journal of Pharmacology*. 134:199–209.
- Perrin, D., and I. G. Sayce. 1967. Computer calculation of equilibrium constants in mixtures of metal ions and complexing species. *Talanta*. 14:833–842.
- Prendergast, F. G., R. P. Haugland, and P. J. Callahan. 1981. 1-[-(Trimethylamino)phenyl]-6-phenylhexa-1,3,5-triene: Synthesis, fluorescence properties, and use as a fluorescence probe of lipid bilayers. *Biochemistry*. 20:7333–7338.
- Smith, R. M., and A. E. Martell. 1982. Critical Stability Constants. Vol 5. Plenum Publishing Co., New York. 604 pp.
- Steinberg, T. H., A. S. Newman, J. A. Swanson, and S. C. Silverstein. 1987. ATP^{4-} permeabilizes the plasma membrane of mouse macrophages to fluorescent dyes. *Journal of Biological Chemistry*. 262:8884–8888.
- Sugiyama, K. 1971. Significance of ATP-splitting activity of rat peritoneal mast cells in the histamine release induced by exogenous ATP. *Japanese Journal of Pharmacology*. 21:531–539.
- Tatham, P. E. R., N. J. Cusack, and B. D. Gomperts. 1990. Characterisation of the ATP^{4-} receptor that mediates permeabilisation of rat mast cells. *European Journal of Pharmacology*. 147:13–21.
- Tatham, P. E. R., and B. D. Gomperts. 1990. Cell permeabilisation. In *Peptide Hormones—A Practical Approach*. Vol. 2. K. Siddle and J. C. Hutton, editors. IRL Press, Oxford. In press.
- Whetton, A. D., S. J. Huang, and P. N. Monk. 1988. Adenosine triphosphate can maintain multipotent hemopoietic stem cells in the absence of interleukin 3 via a membrane permeabilization mechanism. *Biochemical and Biophysical Research Communications*. 152:1173–1178.